J|A|C|S
ARTICLES
Published on Web 07/22/2006

Photocontrolled Magnetization of CdS-Modified Prussian Blue Nanoparticles

Minori Taguchi,[†] Ichizo Yagi,[‡] Masaru Nakagawa,[§] Tomokazu Iyoda,[§] and Yasuaki Einaga*,[†]

Contribution from the Department of Chemistry, Faculty of Science and Technology, Keio University, 3-14-1 Hiyoshi, Kohoku-ku, Yokohama 223-8522, Japan, FC-Cubic, National Institute of Advanced Industrial Science and Technology (AIST), Tokyo Waterfront Center, 2-41-6 Aomi, Koto-ku, Tokyo 135-0064, Japan, and Chemical Resources Laboratory, Tokyo Institute of Technology, 4259 Nagatsuta, Midori-ku, Yokohama 226-8503, Japan

Received May 17, 2006; E-mail: einaga@chem.keio.ac.jp

Abstract: The first photocontrollable magnetic nanoparticles containing CdS and Prussian blue (PB) have been created using reverse micelles as nanoreactors. Photoinduced electron transfer from CdS to PB in the reverse micelle changed the magnetic properties of the composite nanoparticles from ferromagnetic to paramagnetic. The magnetization in the ferromagnetic region below 4 K was substantially decreased after UV light illumination and could be restored almost to its original level by thermal treatment at room temperature. This novel strategy of designing composite nanoparticles containing photoconductive semiconductors and magnetic materials to create photoswitchable magnetic materials may open many possibilities in the development of magneto-optical devices.

Introduction

Optically switchable magnetic materials are becoming increasingly important in the field of high-density information storage.[1] We have been trying to prepare new magnetic materials, the properties of which can be controlled by photoillumination. Our previous work has shown that cobalt−iron cyanide exhibits photoinduced magnetization effects due to an internal electron transfer.[2] However, the number of optically switchable materials reported is still relatively small, since a strategic approach for photoinduced switching in a solid-state system has yet to be established.

To realize the reversible photoswitching of magnetization, we have presented an innovative strategy involving the combination of photochromic molecules with magnetic materials. That is, we have focused on the electrostatic interaction between magnetic materials and photochromic molecules.[3] Although we have demonstrated several photocontrollable magnetic systems, the maximum successful efficiency shown so far for the photoswitching of magnetization was ca. 10%.[3d] This is because there is a limit to the change in the dipole moment that can be caused by the photoisomerization of photochromic molecules, which results in magnetic fields and moments in the composite materials. Therefore, electronic states in magnetic materials were not changed drastically by the photoisomerization of photochromic molecules. If the electronic states of constituent metal ions in magnetic compounds can be directly changed by redox reactions using photoillumination, the magnetic properties can be perfectly photocontrolled, as if by using an on/off switch. In the present work, to create on/off photoswitchable magnetic materials, we have focused on a combination of the photoconductive semiconductor CdS with the magnetic material Prussian blue (PB) at the nanoscale.

Size-tunable optical properties, high photoluminescence quantum yields, large surface areas, and versatility afforded by exchangeable surface-capping molecules have made semiconductor nanoparticles ideal materials for addressing photophysics and chemistry of confined systems as well as for developing novel optical and optoelectronic technologies.[4] In particular, CdS is an *n*-type semiconductor, one of the most fundamentally and technologically important classes of materials.[5,6] With the

[†] Keio University.
[‡] National Institute of Advanced Industrial Science and Technology.
[§] Tokyo Institute of Technology.

(1) (a) Thirion, C.; Wernsdorfer, W.; Mailly, D. *Nat. Mater.* **2003**, *2*, 524. (b) Gütlich, P.; Garcia, Y.; Goodwin, H. A. *Chem. Soc. Rev.* **2000**, *29*, 419.
(2) (a) Sato, O.; Iyoda, T.; Fujishima, A.; Hashimoto, K. *Science* **1996**, *272*, 704. (b) Sato, O.; Einaga, Y.; Iyoda, T.; Fujishima, A.; Hashimoto, K. *J. Electrochem. Soc.* **1997**, *144*, L11. (c) Sato, O.; Einaga, Y.; Fujishima, A.; Hashimoto, K. *Inorg. Chem.* **1999**, *38*, 4405.
(3) (a) Einaga, Y.; Sato, O.; Iyoda, T.; Fujishima, A.; Hashimoto, K. *J. Am. Chem. Soc.* **1999**, *121*, 3745. (b) Taguchi, M.; Li, G.; Gu, Z.-Z.; Sato, O.; Einaga, Y. *Chem. Mater.* **2003**, *15*, 4756. (c) Yamamoto, T.; Umemura, Y.; Sato, O.; Einaga, Y. *Chem. Mater.* **2004**, *16*, 1195. (d) Mikami, R.; Taguchi, M.; Yamada, K.; Suzuki, K.; Sato, O.; Einaga, Y. *Angew. Chem., Int. Ed.* **2004**, *43*, 6135. (e) Taguchi, M.; Yamada, K.; Suzuki, K.; Sato, O.; Einaga, Y. *Chem. Mater.* **2005**, *17*, 4554.
(4) (a) Gaponenko, S. V. *Optical Properties of Semiconductor Nanocrystals*; Cambridge University Press: Cambridge, UK, 1998. (b) Bailey, R. B.; Nie, S. *J. Am. Chem. Soc.* **2003**, *125*, 7100. (c) Medintz, I. L.; Uyeda, T. H.; Goldman, E. R. Mattoussi, H. *Nat. Mater.* **2005**, *4*, 435. (d) Alivisatos, A. P. *Science* **1996**, *271*, 933. (e) Ashoori, R. *Nature* **1996**, *379*, 413. (f) Shim, M.; Guyot-Sionnest, P. *Nature* **2000**, *407*, 981. (g) Wang, C.; Shim, M.; Guyot-Sionnest, P. *Science* **2001**, *291*, 2390.
(5) (a) Pan, D.; Jiang, S.; An, L.; Jiang, B. *Adv. Mater.* **2004**, *16*, 982. (b) Yu, Z.; Li, J.; O'Connor, D. B.; Wang, L.-W.; Barbara, P. F. *J. Phys. Chem. B* **2003**, *107*, 5670. (c) Yu, W. W.; Peng, X. *Angew. Chem., Int. Ed.* **2002**, *41*, 2368. (d) Rockenberger, J.; Tröger, L.; Kornowski, A.; Vossmeyer, T.; Eychmüller, A.; Feldhaus, J.; Weller, H. *J. Phys. Chem. B* **1997**, *101*, 2691. (e) Cao, Y. C.; Wang, J. *J. Am. Chem.* Soc. **2004**, *126*, 14336.
(6) Harruff, B. A.; Bunker, C. E. *Langmuir* **2003**, *19*, 893.

10.1021/ja063461e CCC: $33.50

emergence of CdS nanoparticles that demonstrate properties lying between the molecular and bulk limits, a number of striking effects, such as size quantization, nonlinear optical behaviors, and unusual fluorescence, have been explored. On the other hand, PB is a long-known pigment recognized as a functional inorganic material,[7,8] which possesses a face-centered cubic (fcc) lattice of iron ion centers bridged by electron-rich cyanide groups. Superior attractive magnetic functions, such as photomagnetism[2,9a] and ferromagnetism at room temperature,[9b] were also observed by changing the iron atoms of PB to other transition metals. Furthermore, interest in the synthesis of PB and its analogue particles at the nanoscale[10,11] has emerged recently because of their unique properties.

Another important point in the present work is that we have adopted reverse micelles as nanoreactors to prepare the composite nanoparticles.[12] Reverse micelles (water-in-oil (w/o) nanoemulsions) can easily produce monodispersed colloid nanoparticles, which are essential for studying the size dependence of physical properties at the nanoscale. In a reverse nanoemulsion, the aqueous phase is dispersed as nanodroplets are stabilized by a monolayer of surfactant molecules in the continuous hydrocarbon phase. Furthermore, reactions in reverse nanoemulsions as nanoreactors have attracted considerable attention recently, as the numerous nanodroplets of water domains are deemed to be ideal media to prepare nanoparticles with good stability.

Recently, there have been a few reports of formation of bifunctional dimer nanocrystals wherein two nanocrystals of different inorganic compositions are fused together.[13] Metal−metal (FePt−Ag),[13a] metal−semiconductor (FePt−CdS),[13b] metal oxide−semiconductor (γ-Fe_2O_3−CdS),[13c] and metal oxide−metal−semiconductor (Fe_3O_4−Au−PbS)[13d] junctions in nanocrystal heterostructures have been shown. However, in those reports, the focus has been on the technique for the preparation of the dimer nanocrystals, with very little discussion of the functional properties, such as photoresponsive physicochemical ones. Furthermore, photocontrollable magnetization has never been reported. Here, to create on/off photoswitchable magnetic nanoparticles, we have designed a new system containing CdS and PB using reverse micelles as nanoreactors. As a result, the novel phenomenon of on/off photoswitching of magnetization was observed in this system.

(7) (a) Robin, M. B. *Inorg. Chem.* **1962**, *1*, 337. (b) Buser, H. J.; Schwarzenbach, D.; Petter, W.; Ludi, A. *Inorg. Chem.* **1977**, *16*, 2704. (c) Herren, F.; Fischer, P.; Ludi, A.; Hälg, W. *Inorg. Chem.* **1980**, *19*, 956.
(8) (a) Itaya, K.; Uchida, I. *Inorg. Chem.* **1986**, *25*, 389. (b) DeLongchamp, D. M.; Hammond, P. T. *Adv. Funct. Mater.* **2004**, *14*, 224.
(9) (a) Li, G.; Akitsu, T.; Sato, O.; Einaga, Y. *J. Am. Chem. Soc.* **2003**, *125*, 12396. (b) Ferlay, S.; Mallah, T.; Ouahès, R.; Veillet, P.; Verdaguer, M. *Nature* **1995**, *378*, 701.
(10) (a) Vaucher, S.; Li, M.; Mann, S. *Angew. Chem., Int. Ed.* **2000**, *39*, 1793. (b) Uemura, T.; Kitagawa, S. *J. Am. Chem. Soc.* **2003**, *125*, 7814. (c) Uemura, T.; Ohba, M.; Kitagawa, S. *Inorg. Chem.* **2004**, *43*, 7339. (d) Dominguez-Vera, J. M.; Colacio, E. *Inorg. Chem.* **2003**, *42*, 6983.
(11) (a) Vaucher, S.; Fielden, J.; Li, M.; Dujardin, E.; Mann, S. *Nano. Lett.* **2002**, *2*, 225. (b) Catala, L.; Gacoin, T.; Boilot, J.-P.; Rivière, É.; Paulsen, C.; Lhotel, E.; Mallah, T. *Adv. Mater.* **2003**, *15*, 826. (c) Yamada, M.; Arai, M.; Kurihara, M.; Sakamoto, M.; Miyake, M. *J. Am. Chem. Soc.* **2004**, *126*, 9482.
(12) (a) Fendler, J. H. *Membrane Mimetic Chemistry*; Wiley: New York, 1982. (b) Lal, M.; Kumar, N. D.; Joshi, M. P.; Prasad, N. *Chem. Mater.* **1998**, *10*, 1065. (c) Ingert, D.; Pileni, M. P. *Adv. Funct. Mater.* **2001**, *11*, 136.
(13) (a) Gu, H.; Yang, Z.; Gao, J.; Chang, C. K.; Xu, B. *J. Am. Chem. Soc.* **2005**, *127*, 34. (b) Gu, H.; Zheng, R.; Zhang, X.; Xu, B. *J. Am. Chem. Soc.* **2004**, *126*, 5664. (c) Kwon, K.-W.; Shim, M. *J. Am. Chem. Soc.* **2005**, *127*, 10269. (d) Shi, W.; Zeng, H.; Sahoo, Y.; Ohulchanskyy, T. Y.; Ding, Y.; Wang, Z. L.; Swihart, M.; Prasad, P. N. *Nano Lett.* **2006**, *6*, 875.

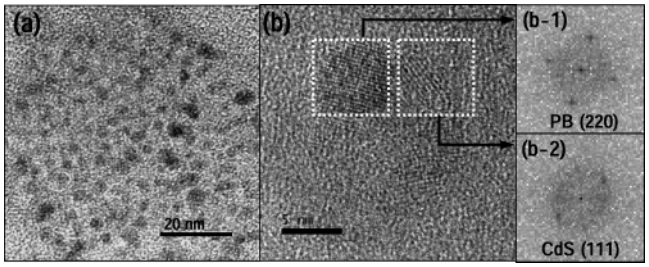

Figure 1. (a) TEM images of **1**. (b) TEM image of heterostructure for CdS-modified PB nanoparticles in **1**. FFT diffraction patterns of selected areas for (b-1) PB and (b-2) CdS in **1**.

Experimental Section

Synthesis of PB, CdS, and CdS-Modified PB Nanoparticles. Didodecyldimethylammonium bromide (DDAB) was purchased from Aldrich. $FeCl_2 \cdot 4H_2O$, $K_3[Fe(CN)_6]$, $CdCl_2$, $Na_2S \cdot 9H_2O$, and toluene were purchased from Wako. DDAB (5 mmol) was first dissolved in toluene (50 mL, 0.1 M). $FeCl_2 \cdot 4H_2O$ ($CdCl_2$) (45 μmol) was added to the DDAB solution. The mixture was sonicated until the entire solid disappeared and a clear yellow reverse-micelle solution was obtained. $K_3[Fe(CN)_6]$ ($Na_2S \cdot 9H_2O$) was dissolved separately in deionized water (0.1 M). The $K_3[Fe(CN)_6]$ solution ($Na_2S \cdot 9H_2O$ solution) was slowly added to the reverse-micelle solution at room temperature to produce the DDAB w/o nanoemulsions at $w = 5$ with vigorous stirring. The PB nanoemulsion changed from a transparent yellow solution to a transparent blue solution at once, and no precipitate was observed for one week. The CdS nanoemulsion was synthesized in same way as the PB nanoemulsion. The CdS nanoemulsion changed from a transparent solution to a transparent yellow solution at once, and no precipitate was observed for one week. The PB nanoemulsion was mixed with the CdS nanoemulsion at a volume ratio of 1 (PB/CdS = 1). Figure S1 (Supporting Information) shows a schematic illustration of the synthesis of the composite nanoparticles using reverse nanoemulsions as nanoreactors. Hereafter, the composite nanoparticles are designated as **1**. Films of **1** were then prepared by casting the above solutions onto substrates.

Physical Methods. UV−visible absorption spectra were recorded on a V-560 spectrophotometer (JASCO), and IR (Fourier transform infrared spectrometer) absorption spectra were recorded on an FT/IR-660 Plus (JASCO). A field emission transmission electron microscope (FE-TEM, TECNAI F20, Philips) was used to image the composite materials. The magnetic properties were investigated using a superconducting quantum interference device magnetometer (SQUID, MPMS-XL, Quantum Design). UV illumination (filtered light, $\lambda_{max} = 360$ nm, 1.0 mW cm^{-2}) was applied using an ultra-high-pressure mercury lamp (SP-7 SPOT CURE, USHIO). Similarly, visible light illumination (400−700 nm, 1.0 mW cm^{-2}) was applied using a xenon lamp (XFL-300, Yamashita Denso). ^{57}Fe Mössbauer spectra were measured at room temperature and at low temperature by using a Topologic Systems model 222 constant-acceleration spectrometer with a ^{57}Co/Rh source in transmission mode. When we measured the spectra at low temperature, a closed-cycle helium refrigerator (Nagase Electronic Equipments Service Co., Ltd.) was used.

Results and Discussion

Characterization of Composite Nanoparticles. The TEM image of **1** shows the presence of nanoparticles (Figure 1a). Although the composite nanoparticles were, to some extent, sensitive to the electron beam, lattice fringes for PB and CdS in **1** and fast-Fourier-transform (FFT) diffraction patterns of selected areas for **1** were observed and are shown, along with the simulated FFT, in Figure 1b. From the measured *d* spacing, (220) and (111) were assigned to the observed lattice fringes

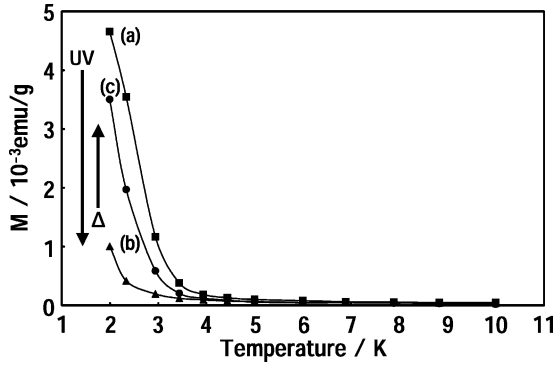

Figure 2. Field-cooled magnetization (FCM) curves for **1** before and after UV light illumination at $H = 1$ mT, (a, ■) before illumination, (b, ▲) after UV light illumination for 10 min, and (c, ●) after thermal treatment at room temperature.

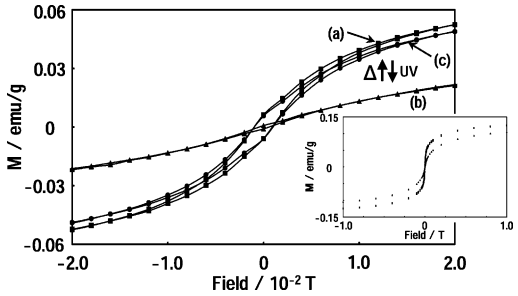

Figure 3. Field dependence of the magnetization for **1** before and after UV light illumination at 2 K. Hysteresis loops for **1** at 2 K, (a, ■) before illumination, (b, ▲) after UV light illumination for 10 min, and (c, ●) after thermal treatment at room temperature.

for PB[7b,10a−c] and CdS,[5,13b,c] respectively. We have also characterized both PB and CdS nanoparticles. The observed average diameter was 4.33 ± 0.71 and 4.44 ± 1.06 nm, respectively, and the observed FFT diffraction patterns exhibit lattice fringes for PB and CdS (Figures S2 and S3, Supporting Information). Furthermore, the PB and CdS nanoparticles were characterized by spectroscopic methods (Figures S4 and S5, Supporting Information).

Magnetic Properties of Photofunctional Composite Nanoparticles. The magnetic properties of **1** were measured by SQUID. The field-cooled magnetization (FCM) was measured as a function of temperature (Figure 2). Ferromagnetic behavior was observed below ca. 4 K (Curie temperature, T_C) before illumination (Figure 2a). In general, bulk PB exhibits ferromagnetic behavior below a T_C of 5.5 K.[7c] The observed lower T_C was consistent with the size-dependence of the PB particles, resulting from an increase in the surface-to-volume ratio with a decrease in the nanoparticle size.[10b,c] After UV light illumination for 10 min at 2 K under a magnetic field of 1 mT, the magnetization value substantially decreased from 4.66×10^{-3} to 1.00×10^{-3} emu/g (Figure 2b). Even after UV light illumination was terminated, this decreased magnetization was maintained for at least 12 h at 2 K. After thermal treatment at room temperature in air, the magnetization value at 2 K under a magnetic field of 1 mT was restored to 3.50×10^{-3} emu/g (Figure 2c). Furthermore, the field dependence of the magnetization at 2 K showed a hysteresis loop ($M_r = 6.35 \times 10^{-2}$ emu/g and $H_c = 1$ mT) before UV light illumination (Figure 3a). After UV light illumination for 10 min at 2 K under a magnetic field of 1 mT, the hysteresis loop disappeared (Figure 3b), and it was restored after thermal treatment at room temperature in air (Figure 3c). On the other hand, the magnetic properties of bulk PB, surfactant (DDAB), the PB nanoparticles, and the CdS nanoparticles individually were not changed by photoillumination.

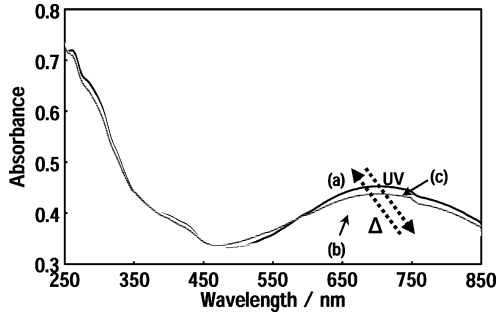

Figure 4. Changes in the optical absorption spectra for **1** with UV light illumination at room temperature. The spectra were recorded during the illumination from $t = 0$ min to $t = 10$ min at 1 min intervals, (a) before illumination, (b) after UV light illumination for 10 min, and (c) after thermal treatment at room temperature.

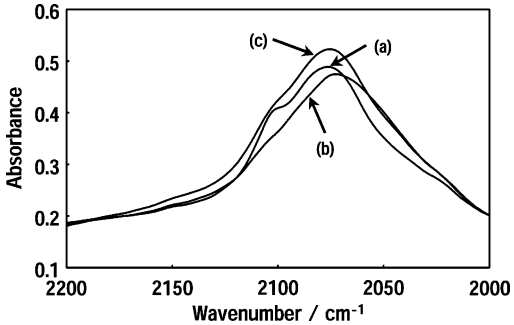

Figure 5. Changes in the IR spectra for **1** with UV light illumination at room temperature. The spectra were recorded during the illumination from $t = 0$ min to $t = 10$ min at 1 min intervals (a) before illumination, (b) after UV light illumination for 10 min, and (c) after thermal treatment at room temperature.

Photoinduced Electron Transfer from CdS to PB in Composite Nanoparticles. We have focused on the interaction between PB and CdS in **1** in order to understand the mechanism of photoinduced magnetic phenomena. To investigate the photoinduced electron transfer from CdS to PB in **1**, we monitored the intervalence charge-transfer (IVCT ($Fe^{II}-CN-Fe^{III}$)) band, CN stretching (ν(CN)), and electronic states of the iron atoms via UV−visible, IR, and ^{57}Fe Mössbauer spectroscopy, respectively, of the PB in **1** with UV light illumination.

First, the UV−visible absorption spectrum at room temperature before illumination is shown in Figure 4a. The absorption edge at 450 nm is ascribed to the band gap (2.76 eV) of CdS, and the broad band at 696 nm (λ_{max}) is consistent with the IVCT band of PB in **1**. After UV light illumination for 10 min, the absorbance of the IVCT band decreased (Figure 4b). Itaya et al.[8a] and Hammond et al.[8b] described the electrochromic color change of PB. According to them, absorbance at 700 nm, assigned to the IVCT band of PB, was observed (electronic states of $Fe^{II}-CN-Fe^{III}$) at an electrode potential of 0.6 V (vs SCE), while no distinct bands were observed in the visible region when it was reduced to −0.2 V ($Fe^{II}-CN-Fe^{II}$). Second, the frequencies of CN stretching, ν(CN), of **1**, showed a peak at 2076 cm^{-1} and a shoulder at 2100 cm^{-1} before illumination at room temperature (Figure 5a). The strong peak at 2076 cm^{-1} is ascribed to the ν(CN) of the $Fe^{II}-CN-Fe^{III}$ bridge.[14] The observation of the shoulder at 2100 cm^{-1}, indicating the

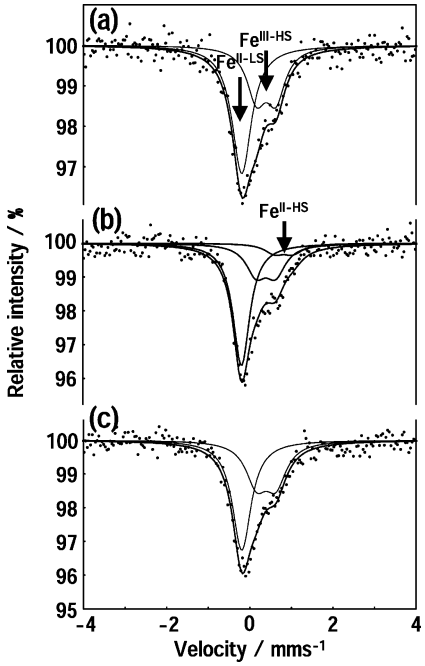

Figure 6. ^{57}Fe Mössbauer spectrum for **1** before and after UV light illumination at 9 K, (a) before illumination, (b) after UV light illumination for 10 min, and (c) after thermal treatment at room temperature.

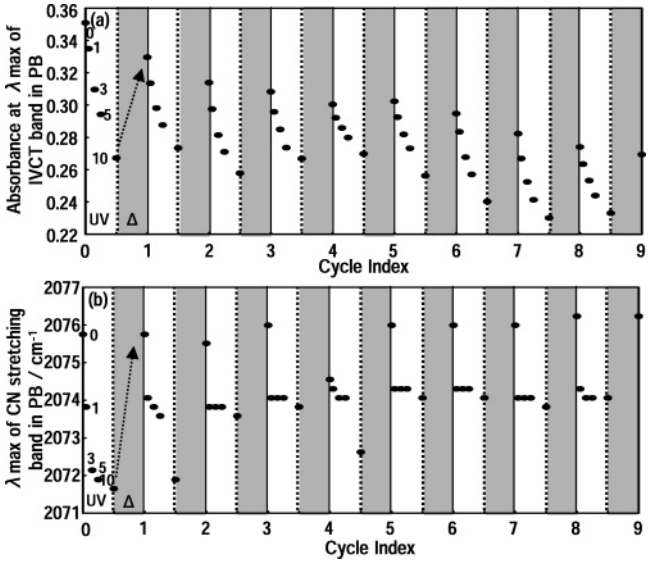

Figure 7. Changes in (a) the absorbance at λ_{max} of the IVCT band and (b) the CN stretching band in IR spectra of **1** upon UV light illumination and thermal treatment at room temperature in air. These spectra were recorded during the illumination from $t = 0$ min to $t = 10$ min at 1 min intervals (white area) and again after thermal treatment at room temperature in air (gray area). The 10 min UV illumination and the thermal treatment were repeated nine times.

presence of terminal CN groups on the PB surface, also suggests the formation of nanoparticles in the reverse micelle. After UV light illumination, the value of ν(CN) shifted from 2076 to 2072 cm^{-1} and the shoulder peak at 2100 cm^{-1} decreased (Figure 5b). It is possible that the peak shift is due to the photoinduced reduction of the PB from $Fe^{II}-CN-Fe^{III}$ to $Fe^{II}-CN-Fe^{II}$ and the decrease of the shoulder at 2100 cm^{-1} is due to an interaction between CdS and PB in **1**, such as formation of chemical bond at the interface. That is, these spectral changes with UV light illumination suggest electron transfer from CdS to PB in **1**. Similar results for UV−visible and IR measurements were also obtained at 8 K (Figures S6 and S7, Supporting Information). Finally, the ^{57}Fe Mössbauer spectra at 9 K support these assignments (Figure 6). Before illumination, a doublet absorption peak (isomer shift, IS = 0.393 mm/s; quadrupole splitting, QS = 0.467 mm/s), which was assigned to Fe^{III-HS}, and a singlet absorption peak (IS = − 0.193 mm/s), which was assigned to Fe^{II-LS}, were observed.[14] The Fe^{III-HS}/Fe^{II-LS} ratio was estimated to be 57.3/42.7 (Figure 6a). After UV light illumination, in addition to both Fe^{III-HS} and Fe^{II-LS}, a new doublet absorption peak was observed (IS = 0.821 mm/s, QS = 0.442 mm/s), which was assigned to Fe^{II-HS}. The $Fe^{III-HS}/Fe^{II-LS}/Fe^{II-HS}$ ratio changed to 32.2/57.5/10.3 (Figure 6b). This is consistent with the photoinduced reduction of the PB from $Fe^{II}-CN-Fe^{III}$ to $Fe^{II}-CN-Fe^{II}$. The UV−visible, IR, and ^{57}Fe Mössbauer spectra were restored to the original spectra after thermal treatment at room temperature in air. That is, the reduced PB was oxidized in air at room temperature. The back electron transfer easily occurred at room temperature in air, although the reduced $Fe^{II}-CN-Fe^{II}$ state can be maintained for several hours, even at room temperature. The cycle (UV-induced charge transfer and thermally induced back reaction) was repeated several times by UV−visible and IR measurements in the solid state at room temperature (Figure 7). In fact, the reverse reaction (oxidation process) occurred very easily at room temperature, especially in air. However, when the $Fe^{II}-CN-Fe^{II}$ state was annealed to room temperature in vacuo, the efficiency of the reverse reaction decreased. Furthermore, when the state was kept in vacuo at low temperature, the lifetime was longer (at least 12 h). Studies on the detailed kinetics of the reaction and mechanisms are now in progress.

On the other hand, interestingly, **1** did not show photoluminescence by UV and visible light illumination, although the CdS nanoparticles show strong photoluminescence with UV light illumination at room temperature (Figure S8, Supporting Information). It was suggested that the quenching of photoluminescence in **1** was also consistent with the electron transfer from CdS to PB in **1**. Moreover, when the PB nanoparticles without CdS encapsulated with DDAB were illuminated with UV and visible light, no changes were observed in UV−visible, IR, and ^{57}Fe Mössbauer spectroscopy. Therefore, these results suggested that the CdS in **1** plays an important role in the photocontrolled magnetization of **1**.

Mechanism of Photocontrollable Magnetization. Sato et al. described the magnetic properties of PB depending on its electronic states. They prepared them by an electrochemical method.[15] For example, when PB is oxidized or reduced electrochemically, the magnetic properties change progressively. This modification of the magnetic properties arises mainly from changes in the degree of valence delocalization. The electrons in the PB that formerly occupied the t_{2g} orbital on the $Fe^{II-LS}(t_{2g}^6 e_g^0)$ are partly delocalized onto the neighboring $Fe^{III-HS}(t_{2g}^3 e_g^2)$. Since the t_{2g} and e_g orbitals of the Fe^{III-HS} are both exactly half occupied, it is energetically favorable to delocalize only one type of spin (α or β spin) from the Fe^{II-LS} to the Fe^{III-HS} due to the coulomb and exchange repulsion terms.

(14) Reguera, E.; Fernández-Bertrán, J.; Balmaseda, J. *Transition Met. Chem.* **1999**, *24*, 648.

(15) Sato, O.; Hayami, S.; Einaga, Y.; Gu, Z.-Z. *Bull. Chem. Soc. Jpn.* **2003**, *76*, 443.

The spin polarization on the Fe^{II-LS} induces a magnetic correlation with the Fe^{III-HS}, leading to magnetic ordering at 4.2 K. After reduction, the electronic state is converted to $Fe^{II-LS}(t_{2g}^6 e_g^0)-CN-Fe^{II-HS}(t_{2g}^4 e_g^2)$, and hence partial delocalization of the electrons from the Fe^{II-LS} to the Fe^{II-HS} (or vice versa) is prevented due to large coulomb repulsion. Thus, the spin polarization on the Fe^{II-LS} almost disappears, which results in reduction of the magnetic interaction between the Fe^{II-HS} and the Fe^{II-LS}. As a consequence, the compound shows ferromagnetic-to-paramagnetic interconversion upon electrochemical reduction. With regard to the magnetic properties, the photoinduced change observed in the present work, shown in Figures 2 and 3, which was due to the photoinduced reduction of PB from $Fe^{II}-CN-Fe^{III}$ to $Fe^{II}-CN-Fe^{II}$, is the same as the change resulting from the electrochemical reduction of PB. Furthermore, when the PB is oxidized to $Fe^{III}_4[Fe^{III}(CN)_6]_3$, T_C progressively increases. This is consistent with the fact that the diamagnetic component, $Fe^{II-LS}(t_{2g}^6 e_g^0)$, is oxidized to $Fe^{III-LS}(t_{2g}^5 e_g^0)$ with one unpaired electron in the t_{2g} orbital.

Conclusion

CdS-modified PB nanoparticle heterojunctions can be formed using reverse micelles as nanoreactors. The formation of CdS-modified PB heterojunctions in the reverse micelle shows photoinduced electron transfer form CdS to PB. As a result, we can change the magnetic properties of the composite nanoparticles in the solid state. That is, we succeeded in introducing photofunctionality to molecule-based magnetic materials at the nanoscale. The present work will supply the novel strategy to create photoswitchable magnetic materials.

Acknowledgment. This work was supported by a Grant-in-Aid for Scientific Research on Priority Areas (417) and the 21st Century COE program "KEIO Life Conjugate Chemistry" from the Ministry of Education, Culture, Sports, Science and Technology (MEXT) of the Japanese Government.

Supporting Information Available: Schematic illustration of the synthesis of **1**, and characterization (TEM images; UV−visible, IR, ^{57}Fe Mössbauer, and photoluminescence spectra) of **1**, the PB nanoparticles, and the CdS nanoparticles This material is available free of charge via the Internet at http://pubs.acs.org.

JA063461E

Supporting Information Available for "Photo-controlled Magnetization of CdS-Modified Prussian Blue Nanoparticles"

Minori Taguchi,[†] *Ichizo Yagi*,[‡] *Masaru Nakagawa*,[§] *Tomokazu Iyoda*,[§] and *Yasuaki Einaga*[†]*

Department of Chemistry, Faculty of Science and Technology, Keio University, 3-14-1 Hiyoshi, Kohoku-ku, Yokohama 223-8522, Japan

[†]Keio University

[§]AIST

[‡]Tokyo Institute of Technology

Supporting Figures

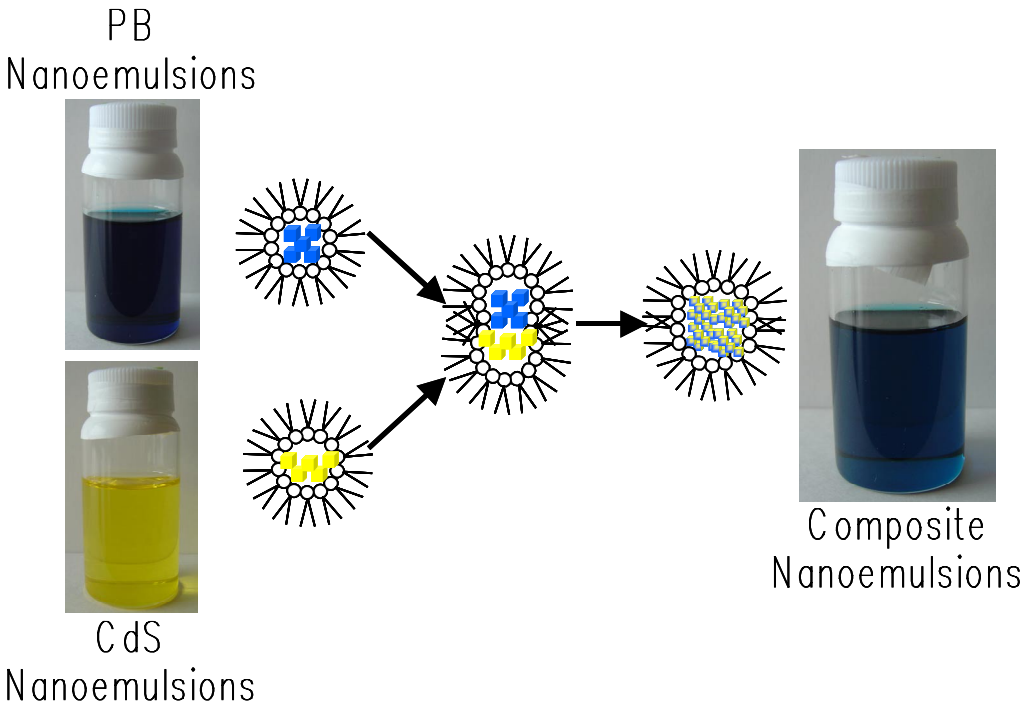

Figure S1. Schematic illustration of the synthesis of composite nanoparticles using reverse nanoemulsions as nanoreactor.

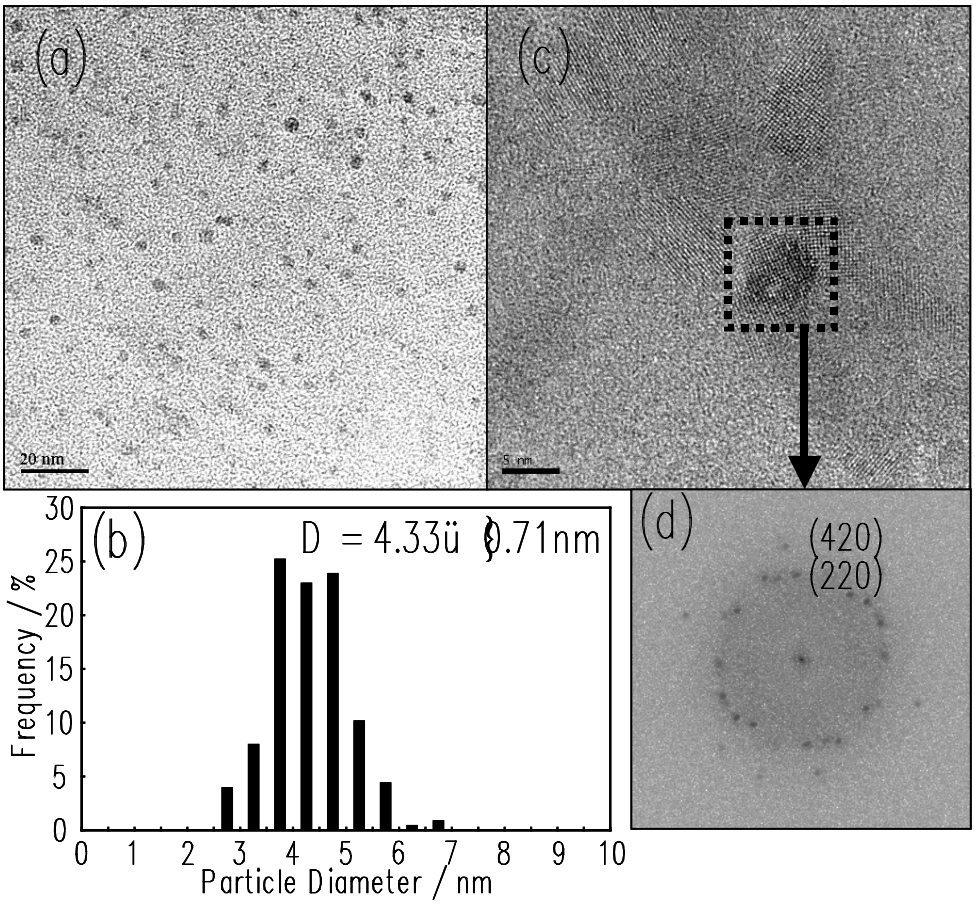

Figure S2. (a) TEM image, (b) size distribution, and (c) TEM image of superlattices of the PB nanoparticles, respectively. (d) FFT diffraction patterns of selected area for the PB from the TEM image of (c).

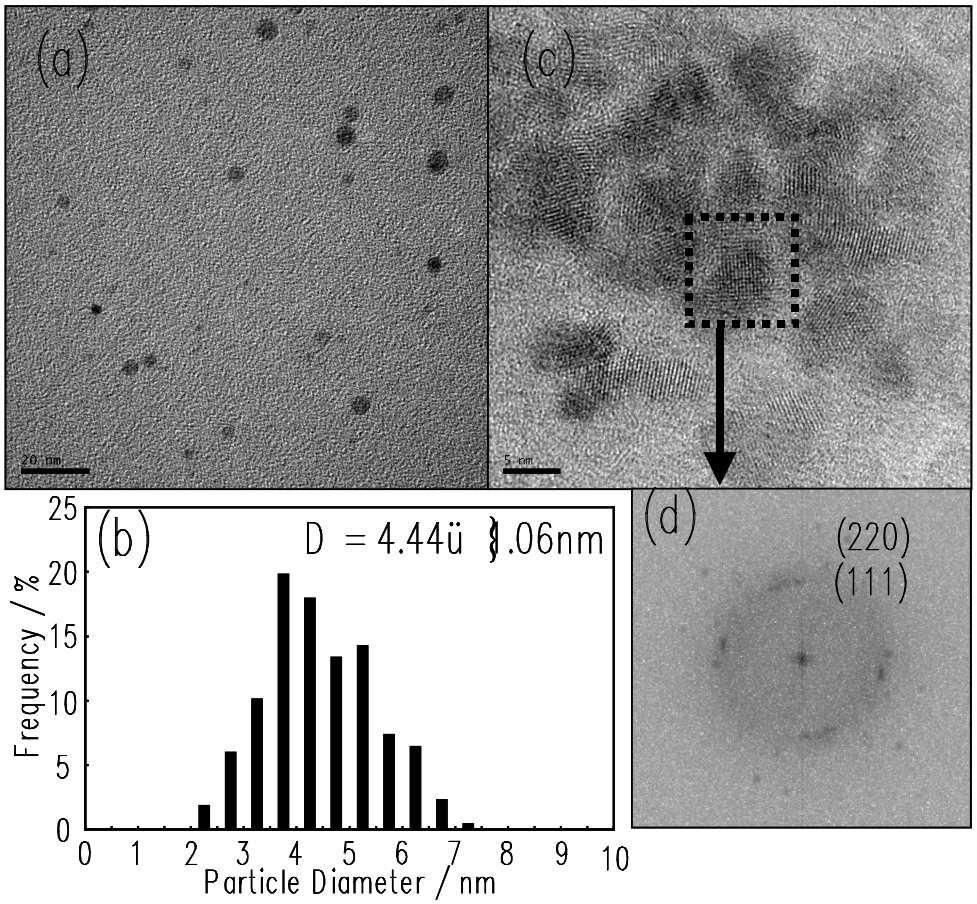

Figure S3. (a) TEM image, (b) size distribution, and (c) TEM image of superlattices of the CdS nanoparticles, respectively. (d) FFT diffraction patterns of selected area for the CdS from the TEM image of (c).

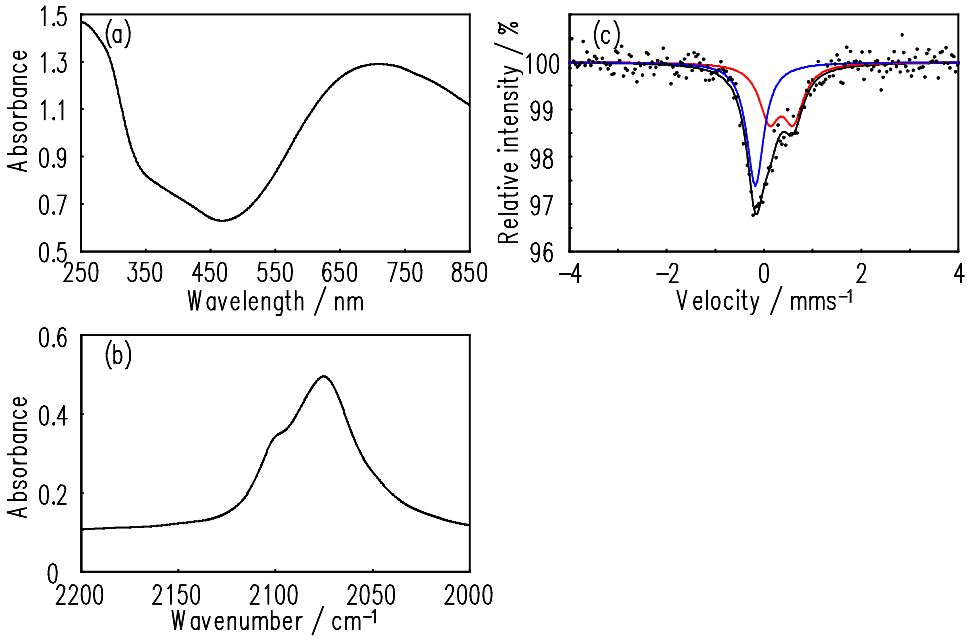

Figure S4. (a) UV-visible and (b) IR absorption spectrum for the PB nanoparticles in solid state at room temperature. (c) ^{57}Fe Mössbauer spectrum for the PB nanoparticles in solid state at 9 K.

The IVCT band in PB was obtained at 711 nm (λ_{max}) by UV-visible spectrum.[7a] IR spectrum showed that the strong peak at 2073 cm^{-1} and shoulder at 2100 cm^{-1} are the ν(CN) of Fe^{II}-CN-Fe^{III} bridge and the presence of terminal CN groups on the PB nanoparticle surface.[14] ^{57}Fe Mössbauer spectrum showed that a doublet absorption peak (IS = 0.373 mm/s, QS = 0.432 mm/s), which was assigned to $Fe^{III\text{-}HS}$, and a singlet absorption peak (IS = - 0.177 mm/s), which was assigned to $Fe^{II\text{-}LS}$ were observed. The $Fe^{III\text{-}HS}$ / $Fe^{II\text{-}LS}$ ratio was estimated to be 50.3 / 49.7.[14] These spectra indicate the presence of PB.

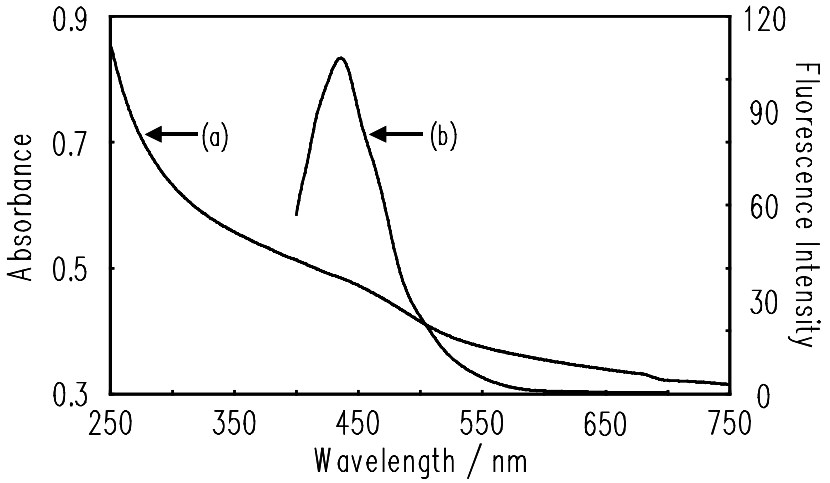

Figure S5. (a) UV-visible and (b) photoluminescence emission spectra (λ_{ex} = 380 nm) of the CdS nanoparticles in solid state at room temperature.

The UV-visible spectrum is characteristic the CdS nanoparticles, with a distinct exciton shoulder and an absorption edge at 500 nm that is blue-shifted with respect to bulk CdS. The fluorescent spectra of the CdS nanoparticles show an emission maximum at 435 nm, which is also consistent with the value in the literature of corresponding CdS nanocrystals.[6]

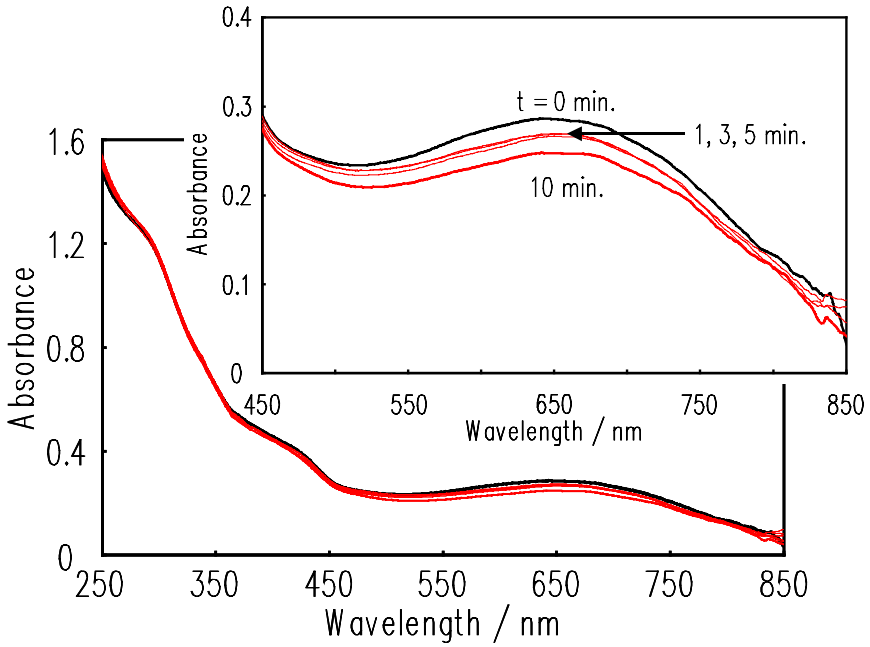

Figure S6. Changes in the optical absorption spectra for **1** with UV light illumination at 8 K. The spectra were recorded during the illumination from t = 0 min to t = 10 min at 1 min intervals, (black line) before illumination and (red line) after UV light illumination for 10 min.

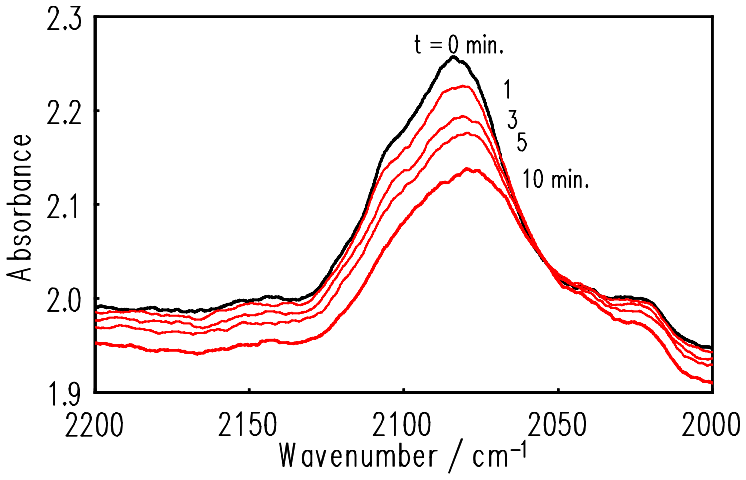

Figure S7. Changes in the IR spectra for **1** with UV light illumination at 8 K. The spectra were recorded during the illumination from t = 0 min to t = 10 min at 1 min intervals (black line) before illumination and (red line) after UV light illumination for 10 min.

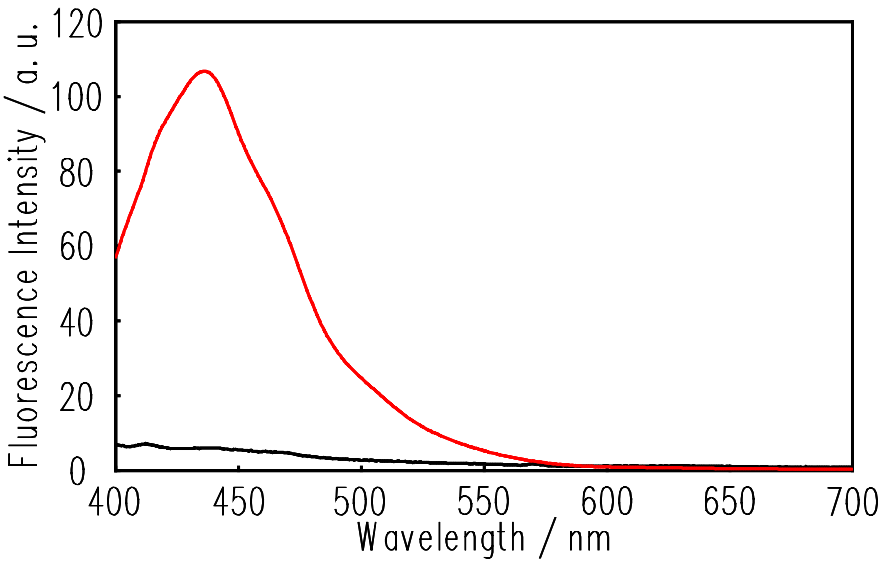

Figure S8. Photoluminescence emission spectra (λ_{ex} = 380 nm) of (black line) **1** and (red line) the CdS in the solid state at room temperature.